JOC Article
pubs.acs.org/joc

Conformational Analysis of *o*-Phenylenes: Helical Oligomers with Frayed Ends

C. Scott Hartley* and Jian He

Department of Chemistry and Biochemistry, Miami University, Oxford, Ohio 45056, United States

scott.hartley@muohio.edu

Received October 23, 2010

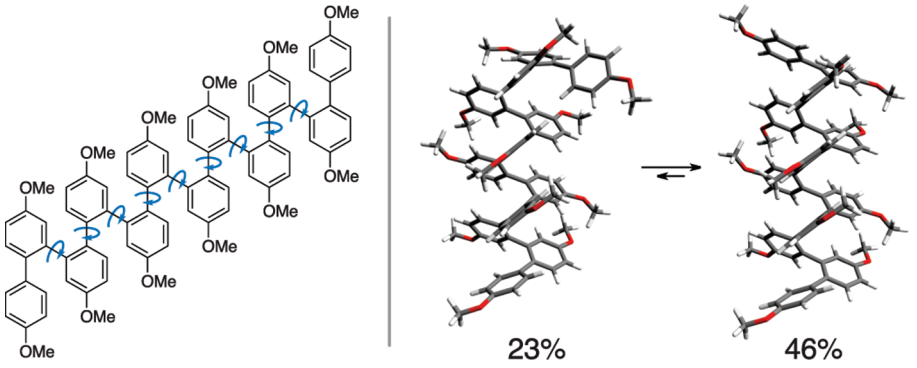

The *o*-phenylenes represent a fundamental class of conjugated polymers that, unlike the isomeric *p*-phenylenes, should exhibit rich conformational behavior. Recently, we reported the synthesis and characterization of a series of *o*-phenylene oligomers featuring unusual electronic properties, including surprisingly long-range delocalization as measured by UV−vis spectroscopy and hypsochromic shifts in fluorescence maxima with increasing length. To rationalize these properties, we hypothesized that the oligomers predominantly assume a stacked helical conformation in solution. This assertion, however, was supported by only indirect evidence. Here we present a thorough investigation of the conformational behavior of this series of *o*-phenylenes by dynamic NMR spectroscopy and computational chemistry. EXSY experiments, in combination with other two-dimensional NMR techniques, provided full ^{1}H chemical shift assignments for at least the two most prevalent conformers for each member of the series (hexamer to dodecamer). GIAO density functional theory calculations were then used to relate the NMR data to specific molecular geometries. We have found that the *o*-phenylenes do indeed assume stacked helical conformations with disorder occurring at the ends. Thus, the *o*-phenylene motif appears to have great potential as a means to organize arenes into predictable three-dimensional arrangements. Our results also illustrate the power of ^{1}H NMR GIAO predictions in the solution-phase conformational analysis of oligomers, particularly those with a high density of aromatic subunits.

Introduction

Oligomers and polymers with well-defined secondary structures have attracted considerable attention as analogues of biological macromolecules and for applications in materials science and nanotechnology.[1] These systems generally exploit intramolecular forces (e.g., hydrogen bonding, π-stacking), amphiphilicity, or backbone torsional biases to promote the formation of specific conformations. The design and synthesis of such molecules is currently of great interest, especially if their conformational behavior can be coupled to interesting properties or functions. Thus, oligomeric or polymeric architectures have been developed exhibiting molecular recognition,[2] chiroptical properties,[3] mechanical actuation,[4]

(1) (a) Gellman, S. H. *Acc. Chem. Res.* **1998**, *31*, 173–180. (b) Hill, D. J.; Mio, M. J.; Prince, R. B.; Hughes, T. S.; Moore, J. S. *Chem. Rev.* **2001**, *101*, 3893–4011. (c) Cornelissen, J. J. L. M.; Rowan, A. E.; Nolte, R. J. M.; Sommerdijk, N. A. J. M. *Chem. Rev.* **2001**, *101*, 4039–4070. (d) *Foldamers: Structure, Properties, and Applications*; Hecht, S., Huc, I., Eds.; Wiley-VCH: Weinheim, 2007. (e) Yashima, E.; Maeda, K.; Iida, H.; Furusho, Y.; Nagai, K. *Chem. Rev.* **2009**, *109*, 6102–6211.

DOI: 10.1021/jo1021025 Published on Web 11/17/2010

unusual modes of reactivity,[5] and catalysis;[6] helical oligomers have also been used as scaffolding to position other functional units.[7] Nevertheless, there remains a need to develop novel structural motifs that exhibit controlled conformational behavior.

Polyphenylene nanostructures are now well-established in organic materials chemistry.[8] The most fundamental members of this class are the *p*-, *m*-, and *o*-phenylene polymers. Of these, the *para* isomers have received by far the most attention, particularly in organic electronics[9] and as molecular wires.[10] Like many conjugated polymers, *p*-phenylenes are essentially rod-like molecules featuring strong through-bond conjugation; however, the connectivity of the *m*- and *o*-phenylenes necessitates that they exhibit much more complex conformational behavior. Accordingly, some *m*-phenylenes have been developed that fold into helical structures.[4c,11] Very little is known about the conformational behavior of the *o*-phenylenes, although some literature reports provide good reasons to suspect that they may be predisposed toward specific helical conformations in solution. For example, Ito and co-workers carried out extensive investigations of the structurally similar poly(2,3-quinoxaline)s (and related structures), establishing a well-defined helical secondary structure for these materials.[12] Similarly, some heterocyclic oligomers, notably oligo(β-pyrrole)s[13] and oligo(α,β-thiophene)s,[14] have been shown to adopt helical conformations. Due to the paucity of reported examples, conformational analysis of actual *o*-phenylenes is significantly less well-developed. However, Simpkins has reported a series of *o*-phenylene oligomers that were shown to adopt a helical structure in the solid state.[15]

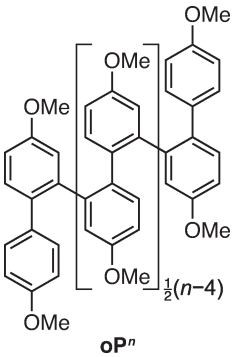

oP^n

As conjugated materials, the *o*-phenylenes in general should exhibit only modest through-bond delocalization due to poor π-overlap along the twisted backbone. However, they provide a very high density of chromophore repeat units and seemed to us to be a promising means to organize them in three dimensions, provided that they adopt conformational states that are both predictable and conveniently characterized. *o*-Phenylenes with well-defined contacts between aromatic monomers could ultimately be used as model systems for the study of through-space effects (e.g., charge transport in DNA) and as novel approaches to molecular wires. Recently, we reported the synthesis and characterization of the homologous series of *o*-phenylene oligomers **oP^n** up to the dodecamer (where *n* indexes the number of repeat units).[16] Access to these compounds allowed us to investigate their electronic structure, revealing several interesting features. As expected, the twisting of the *o*-phenylene backbone leads to a modest overall effect of conjugation in the **oP^n** series, as determined by the total shift in their UV−vis spectra with increasing length. However, small but significant changes in the spectra are observable even for large *n*, giving an effective conjugation length of 8 repeat units. This was surprising given that it had long been suggested that *o*-phenylenes are characterized by

(2) (a) Juwarker, H.; Suk, J.-m.; Jeong, K.-S. *Chem. Soc. Rev.* **2009**, *38*, 3316–3325. (b) Prince, R. B.; Barnes, S. A.; Moore, J. S. *J. Am. Chem. Soc.* **2000**, *122*, 2758–2762. (c) Hou, J.-L.; Shao, X.-B.; Chen, G.-J.; Zhou, Y.-X.; Jiang, X.-K.; Li, Z.-T. *J. Am. Chem. Soc.* **2004**, *126*, 12386–12394. (d) Waki, M.; Abe, H.; Inouye, M. *Angew. Chem., Int. Ed.* **2007**, *46*, 3059–3061. (e) Yamato, K.; Yuan, L.; Feng, W.; Helsel, A. J.; Sanford, A. R.; Zhu, J.; Deng, J. G.; Zeng, X. C.; Gong, B. *Org. Biomol. Chem.* **2009**, *7*, 3643–3647. (f) Ferrand, Y.; Kendhale, A. M.; Kauffmann, B.; Grélard, A.; Marie, C.; Blot, V.; Pipelier, M.; Dubreuil, D.; Huc, I. *J. Am. Chem. Soc.* **2010**, *132*, 7858–7859. (g) Suk, J.-m.; Jeong, K.-S. *J. Am. Chem. Soc.* **2008**, *130*, 11868–11869.

(3) (a) Maeda, K.; Yashima, E. *Top. Curr. Chem.* **2006**, *265*, 47–88. (b) Liu, R.; Shiotsuki, M.; Masuda, T.; Sanda, F. *Macromolecules* **2009**, *42*, 6115–6122. (c) Rivera-Fuentes, P.; Alonso-Gómez, J. L.; Petrovic, A. G.; Santoro, F.; Harada, N.; Berova, N.; Diederich, F. *Angew. Chem., Int. Ed.* **2010**, *49*, 2247–2250.

(4) (a) Kim, H.-J.; Lee, E.; Park, H.-s.; Lee, M. *J. Am. Chem. Soc.* **2007**, *129*, 10994–10995. (b) Percec, V.; Rudick, J. G.; Peterca, M.; Heiney, P. A. *J. Am. Chem. Soc.* **2008**, *130*, 7503–7508. (c) Miwa, K.; Furusho, Y.; Yashima, E. *Nature Chem.* **2010**, *2*, 444–449.

(5) (a) Smaldone, R. A.; Moore, J. S. *J. Am. Chem. Soc.* **2007**, *129*, 5444–5450. (b) Srinivas, K.; Kauffmann, B.; Dolain, C.; Léger, J.-M.; Ghosez, L.; Huc, I. *J. Am. Chem. Soc.* **2008**, *130*, 13210–13211. (c) Hu, H.-Y.; Xiang, J.-F.; Cao, J.; Chen, C.-F. *Org. Lett.* **2008**, *10*, 5035–5038.

(6) (a) Reggelin, M.; Doerr, S.; Klussmann, M.; Schultz, M.; Holbach, M. *Proc. Natl. Acad. Sci. U.S.A.* **2004**, *101*, 5461–5466. (b) Yamamoto, T.; Yamada, T.; Nagata, Y.; Suginome, M. *J. Am. Chem. Soc.* **2010**, *132*, 7899–7901.

(7) (a) Sinkeldam, R. W.; Hoeben, F. J. M.; Pouderoijen, M. J.; De Cat, I.; Zhang, J.; Furukawa, S.; De Feyter, S.; Vekemans, J. A. J. M.; Meijer, E. W. *J. Am. Chem. Soc.* **2006**, *128*, 16113–16121. (b) Wolffs, M.; Delsuc, N.; Veldman, D.; Vân Anh, N.; Williams, R. M.; Meskers, S. C. J.; Janssen, R. A. J.; Huc, I.; Schenning, A. P. H. J. *J. Am. Chem. Soc.* **2009**, *131*, 4819–4829.

(8) (a) Berresheim, A. J.; Müller, M.; Müllen, K. *Chem. Rev.* **1999**, *99*, 1747–1785. (b) Grimsdale, A. C.; Müllen, K. *Macromol. Rapid Commun.* **2007**, *28*, 1676–1702. (c) Schmaltz, B.; Weil, T.; Müllen, K. *Adv. Mater.* **2009**, *21*, 1067–1078.

(9) (a) Ivory, D. M.; Miller, G. G.; Sowa, J. M.; Shacklette, L. W.; Chance, R. R.; Baughman, R. H. *J. Chem. Phys.* **1979**, *71*, 1506–1507. (b) Grem, G.; Leditzky, G.; Ullrich, B.; Leising, G. *Adv. Mater.* **1992**, *4*, 36–37. (c) Kraft, A.; Grimsdale, A. C.; Holmes, A. B. *Angew. Chem., Int. Ed.* **1998**, *37*, 402–428. (d) Grimsdale, A. C.; Müllen, K. *Adv. Polym. Sci.* **2006**, *199*, 1–82. (e) Grimsdale, A. C.; Müllen, K. *Adv. Polym. Sci.* **2008**, *212*, 1–48. (f) Grimsdale, A. C.; Chan, K. L.; Martin, R. E.; Jokisz, P. G.; Holmes, A. B. *Chem. Rev.* **2009**, *109*, 897–1091.

(10) (a) Schlicke, B.; Belser, P.; De Cola, L.; Sabbioni, E.; Balzani, V. *J. Am. Chem. Soc.* **1999**, *121*, 4207–4214. (b) Weiss, E. A.; Ahrens, M. J.; Sinks, L. E.; Gusev, A. V.; Ratner, M. A.; Wasielewski, M. R. *J. Am. Chem. Soc.* **2004**, *126*, 5577–5584. (c) Holman, M. W.; Liu, R.; Zang, L.; Yan, P.; DiBenedetto, S. A.; Bowers, R. D.; Adams, D. M. *J. Am. Chem. Soc.* **2004**, *126*, 16126–16133. (d) Banerjee, M.; Shukla, R.; Rathore, R. *J. Am. Chem. Soc.* **2009**, *131*, 1780–1786.

(11) (a) Goto, H.; Katagiri, H.; Furusho, Y.; Yashima, E. *J. Am. Chem. Soc.* **2006**, *128*, 7176–7178. (b) Goto, H.; Furusho, Y.; Yashima, E. *J. Am. Chem. Soc.* **2007**, *129*, 109–112. (c) Goto, H.; Furusho, Y.; Yashima, E. *J. Am. Chem. Soc.* **2007**, *129*, 9168–9174. (d) Ben, T.; Goto, H.; Miwa, K.; Goto, H.; Morino, K.; Furusho, Y.; Yashima, E. *Macromolecules* **2008**, *41*, 4506–4509.

(12) (a) Ito, Y.; Ihara, E.; Murakami, M. *J. Am. Chem. Soc.* **1990**, *112*, 6446–6447. (b) Ito, Y.; Ihara, E.; Murakami, M. *Angew. Chem., Int. Ed. Engl.* **1992**, *31*, 1509–1510. (c) Ito, Y.; Ohara, T.; Shima, R.; Suginome, M. *J. Am. Chem. Soc.* **1996**, *118*, 9188–9189. (d) Ito, Y.; Miyake, T.; Hatano, S.; Shima, R.; Ohara, T.; Suginome, M. *J. Am. Chem. Soc.* **1998**, *120*, 11880–11893. (e) Suginome, M.; Collet, S.; Ito, Y. *Org. Lett.* **2002**, *4*, 351–354.

(13) Magnus, P.; Danikiewicz, W.; Katoh, T.; Huffman, J. C.; Folting, K. *J. Am. Chem. Soc.* **1990**, *112*, 2465–2468.

(14) (a) Marsella, M. J.; Yoon, K.; Almutairi, A.; Butt, S. K.; Tham, F. S. *J. Am. Chem. Soc.* **2003**, *125*, 13928–13929. (b) Almutairi, A.; Tham, F. S.; Marsella, M. J. *Tetrahedron* **2004**, *60*, 7187–7190. (c) Marsella, M. J.; Rahbarnia, S.; Wilmot, N. *Org. Biomol. Chem.* **2007**, *5*, 391–400.

(15) Blake, A. J.; Cooke, P. A.; Doyle, K. J.; Gair, S.; Simpkins, N. S. *Tetrahedron Lett.* **1998**, *39*, 9093–9096.

(16) He, J.; Crase, J. L.; Wadumethrige, S. H.; Thakur, K.; Dai, L.; Zou, S.; Rathore, R.; Hartley, C. S. *J. Am. Chem. Soc.* **2010**, *132*, 13848–13857.

only very short-range conjugation.[8a,17] The oligomers also exhibit essentially invariant first oxidation potentials and an unusual hypsochromic shift in their fluorescence spectra with increasing length. We attributed these unusual properties to the complex conformational behavior of the *o*-phenylenes compared to most other classes of conjugated oligomers. Specifically, we hypothesized that they adopt a helical solution-phase conformation with offset stacking between every third arene repeat unit, with the long-range delocalization resulting primarily from conformational rigidity. This model provided a solid basis for understanding their behavior but was supported by only indirect evidence. For example, we were able to obtain crystal structures of the shortest oligomers **oP^4** and **oP^6**; however, the longer oligomers did not yield diffraction-quality crystals, and in any event, well-defined solid-state structures certainly would not preclude a complex conformational pool in solution. Further, although the solution-phase UV−vis and fluorescence spectra of the **oP^n** series are consistent with a stacked helical conformation, conclusive evidence was difficult to obtain because the compounds do not undergo controllable conformational changes. Unlike foldamers,[1b] for the **oP^n** series we do not observe transitions from random-coil to ordered conformations and thus do not observe spectral changes that would be more easily interpreted than raw spectra in isolation.

In this paper, we describe direct experimental evidence for stacked helical solution-phase conformations for the **oP^n** series. We begin with a general discussion of their conformational behavior. We then present a thorough NMR investigation of the oligomers, from which we have been able to identify and assign complete sets of ^{1}H chemical shifts for at least the two most-populated conformers of **oP^6**−**oP^{12}**. Using the gauge invariant atomic orbitals (GIAO) method for ab initio predictions of NMR spectra, we have been able to relate the NMR data to specific molecular geometries. This strategy has provided a detailed view of the conformational behavior of these compounds and also should be generalizable to other systems.

Results and Discussion

Conformational Analysis. The key consideration in defining the overall conformational state of an *o*-phenylene is the set of biaryl torsional angles along its backbone. As shown in Figure 1, we label these dihedral angles ϕ_i, where *i* indexes the bonds beginning at one end of the oligomer. Of these, it is only the internal bonds, ϕ_2−ϕ_{n-2}, which must be considered as rotation about the terminal bonds, ϕ_1 and ϕ_{n-1}, is degenerate. In the structurally similar poly(2,3-quinoxaline)s, the ϕ_i assume stable values of approximately ±45° or ±135°.[18] Not surprisingly, we have found that our *o*-phenylenes exhibit similar behavior (see below), although their actual values of ϕ_i are closer to ±70° or ±130° (for ϕ_2−ϕ_{n-2}).

As discussed in our previous paper,[16] the particular conformational state of an *o*-phenylene should have a substantial effect on its properties. The limiting $\phi_i \approx 70°$ conformation is a stacked helix, with close through-space contacts between every third monomer. We call this the "closed" helix, and it

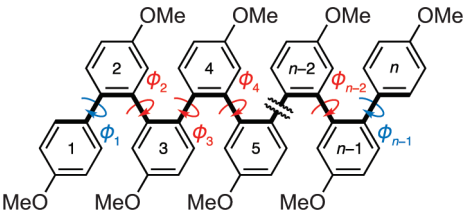

FIGURE 1. Backbone torsional angles ϕ_i and ring numbering for the **oP^n** series. The key degrees of freedom are ϕ_2−ϕ_{n-2} (red). Rotation about the terminal biaryl bonds ϕ_1 and ϕ_{n-1} (blue) is degenerate and thus does not affect the overall conformation of the oligomer. We define each ϕ_i in terms of the four atoms directly along the *o*-phenylene backbone, shown in bold.

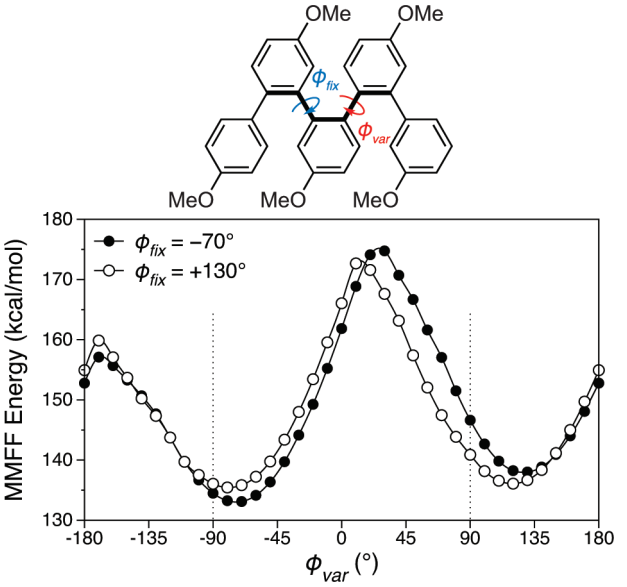

FIGURE 2. MMFF conformational energy profile for rotation about ϕ_{var} with ϕ_{fix} held fixed at −70° or +130° for a model *o*-phenylene pentamer.

corresponds to the conformation observed by Simpkins for his series of *o*-phenylenes in the solid state.[15] We suggested that this conformation best describes the behavior of the **oP^n** series in solution. Conversely, the limiting $\phi_i \approx 130°$ conformation is an elongated, nonstacked helix, which should exhibit more efficient through-bond conjugation. We call this the "open" helix, and it is the state generally (but not always) observed for the poly(2,3-quinoxaline)s and related molecules.[12]

On first consideration, the four distinct torsional states available to each of the biaryl bonds would suggest that the *o*-phenylenes should be predisposed toward intractable mixtures of many interconverting conformers. However, the individual ϕ_i within a particular molecule are *coupled*, simplifying the overall conformational behavior. For example, consider the model *o*-phenylene pentamer in Figure 2, which we studied using the MMFF molecular mechanics method.[19] Although it is a low level of theory, the MMFF method has been found to accurately reproduce the geometries of oligo(α,β-thiophene)s,[14] which are structurally similar to the *o*-phenylenes, and it allows us to consider large numbers of conformers at low computational cost. With the dihedral of

(17) (a) Noren, G. K.; Stille, J. K. *Macromol. Rev.* **1971**, *5*, 385–430. (b) Tour, J. M. *Adv. Mater.* **1994**, *6*, 190–198.
(18) Ito, Y.; Ihara, E.; Murakami, M.; Sisido, M. *Macromolecules* **1992**, *25*, 6810–6813.
(19) *Spartan '08*; Wavefunction, Inc.: Irvine, CA, 2006.

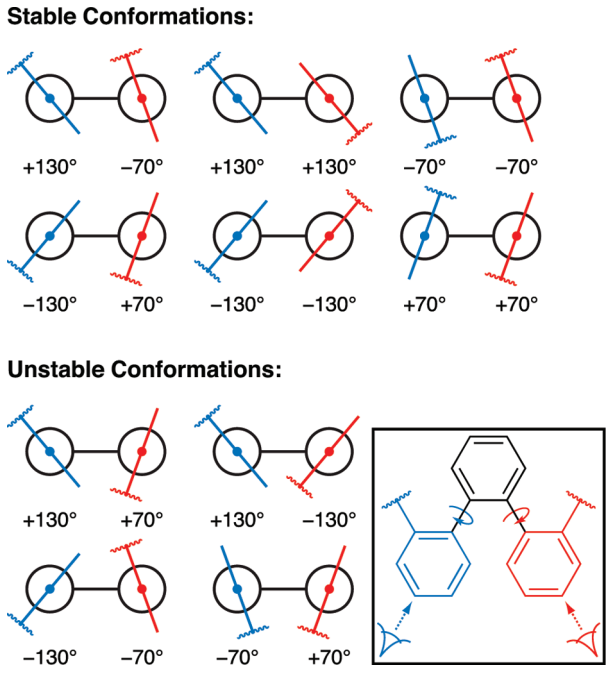

FIGURE 3. Pseudo-Newman projections of a general *o*-phenylene oligomer. The *o*-terphenyl subunit is viewed along the biaryl bonds, which are approximated as parallel for the purpose of the diagram.

one bond held fixed (ϕ_{fix}), we looked at the conformational energy profile for the next bond along the backbone (ϕ_{var}). For each point, a complete conformational search of the other degrees of freedom was carried out in order to avoid memory effects as ϕ_{var} was changed.

When ϕ_{fix} is held at −70°, we find that ϕ_{var} exhibits energy minima at only −70° and +130° (i.e., *not* at +70° or −130°). Likewise, holding ϕ_{fix} at +130° we obtain energy minima at approximately these same values of ϕ_{var}. Thus, rotation about the biaryl bonds in an *o*-phenylene is not independent but depends on the torsional state of other neighboring bonds along the backbone. The reason for this coupling is clear if one considers the different conformations available to an *o*-terphenyl subunit of an *o*-phenylene, for which pseudo-Newman projections are shown in Figure 3. The stable conformations correspond to approximately parallel orientations of the neighboring aromatic rings. Conversely, the unfavorable conformations (+70°/+130°, −70°/−130°, +70°/−70°, and +130°/−130°) correspond to orientations of the neighboring rings that should be destabilized by steric interactions.

As a consequence of this coupling between neighboring biaryl bonds, it follows that, for a single defect-free[20] molecule of any **oP*n***, all of the ϕ_i must be either −70°/+130° or +70/−130°. No individual molecule can incorporate, for example, both a dihedral of +70° and another of −70° at any point along its backbone, since this would require at least one of the unstable conformational states shown in Figure 3. Thus, the overall population of conformers available to *o*-phenylenes can be divided into two enantiomeric pools: −70°/+130° and +70/−130°. To confirm this behavior, we carried

(20) Presumably for an *o*-phenylene polymer there will be a certain frequency of defects along the backbone, but we have no reason to suspect that the relatively short molecules described in this paper are not well below the persistence length.

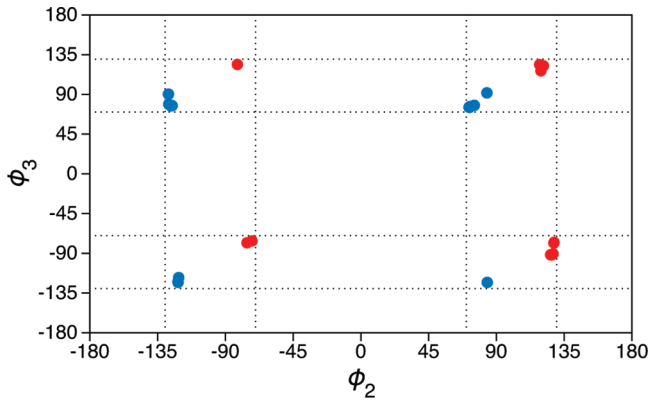

FIGURE 4. Distribution of ϕ_2 and ϕ_3 for **oP^6**, based on a MMFF conformer distribution using 6-fold permutations of ϕ_2−ϕ_4 as starting geometries. Each point represents a stable conformation; the optimized geometries can be divided into two sets: +70°/−130° (blue) and −70°/+130° (red).

out an extensive conformational search for **oP^6** that considered starting geometries from all possible 6-fold permutations of ϕ_2−ϕ_4. In Figure 4, we plot ϕ_3 versus ϕ_2 for the resulting MMFF-minimized conformers. Without exception, the stable conformers fall into either the −70°/+130° or +70/−130° sets.

For simplicity, in the remainder of this paper we will discuss and illustrate the conformational behavior of the **oP*n*** series in terms of the −70°/+130° set, but all of the observed conformers we report are racemic. We name individual conformations as follows: the dihedrals ϕ_2−ϕ_{n-2}, from left to right, are labeled as "A" if they are in the −70° state and "B" if they are in the +130° state. For example, for **oP^8** AAAAA (A_5) refers to the closed helical conformer and BBBBB (B_5) to the open helical conformer.

NMR Spectroscopy and GIAO Calculations. Standard room-temperature ^{1}H NMR spectra of the **oP*n*** series ($n \geq 6$) are complicated by slow conformational exchange on the NMR time scale. This complexity must arise from the different backbone conformers, since the only other degrees of freedom, the orientations of the methoxy groups, should be in rapid exchange. For each oligomer, the overall spectrum is dominated by signals arising from a single 2-fold-symmetric conformer, but additional, smaller signals are also observed that arise from minor conformers. As previously reported, coalescence of the signals is observed at elevated temperatures.[16] All NMR spectra reported in this paper were recorded in $CDCl_3$ at −5 °C, since in some cases this led to a useful sharpening of the peaks.

We begin by discussing the behavior of **oP^6** in detail, since it is a useful illustration of the method used for the other oligomers and it yielded the most comprehensive set of data. Some conclusions can be reached simply by considering the methoxy region of its 1D ^{1}H NMR spectrum (3−4 ppm), shown in Figure 5. Integration, with deconvolution of the overlapping peaks, allows the observed signals to be divided into three sets. The most and least prominent sets comprise three signals each, indicating 2-fold-symmetric conformers we label $\mathbf{I_2}$ and $\mathbf{III_2}$. The remaining set comprises six signals, indicating an unsymmetric conformer we label $\mathbf{II_1}$. Accounting for symmetry, the relative populations of $\mathbf{I_2}$:$\mathbf{II_1}$:$\mathbf{III_2}$ are approximately 55:36:10 based on the peak areas. Analogous

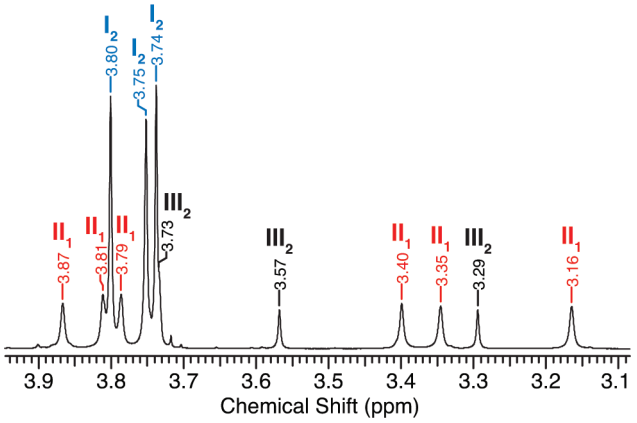

FIGURE 5. Methoxy region of the ^{1}H NMR spectrum of **oP^6** (500 MHz, $CDCl_3$, −5 °C). The signals can be assigned to three individual conformers based on integration. The major conformer, $\mathbf{I_2}$, is 2-fold symmetric. There is one minor unsymmetric conformer, $\mathbf{II_1}$, and another 2-fold-symmetric conformer, $\mathbf{III_2}$.

behavior is observed in the more complex aromatic region of the spectrum (Figure S1 in Supporting Information).

The 2D EXSY (i.e., NOESY) spectrum of **oP^6**, shown in Figure 6 (complete spectrum in Figure S2 in Supporting Information), confirms that these sets of signals do indeed correspond to slowly interconverting conformers. Clear cross peaks are observed between the methoxy groups assigned to the three conformations (Figure 6, right). These cross peaks are of the same phase as the diagonal, indicating that they arise from chemical exchange and not through-space NOE effects[21] given that **oP^6** is a relatively small molecule.[22] Closer inspection of the methoxy region of EXSY spectrum reveals that there are three sets of signals, indicated in Figure 6 by colored arrows, corresponding to the three distinct methoxy groups in **oP^6** (i.e., rings 1/6, 2/5, and 3/4).[23] Each methoxy group can be traced to one signal in each of $\mathbf{I_2}$ and $\mathbf{III_2}$ and two signals in $\mathbf{II_1}$, as expected. Identical behavior is exhibited in the more complex aromatic region of the spectrum (Figure 6, left), i.e., signals for each of the eight aromatic protons can be traced through all three conformers based on the EXSY cross peaks.

The most important function of the EXSY spectrum, however, is that it allowed us to completely assign ^{1}H chemical shifts for each of $\mathbf{I_2}$, $\mathbf{II_1}$, and $\mathbf{III_2}$. Thus, we carried out a standard set of 2D NMR experiments on the same sample of **oP^6**, including DQFCOSY, HMQC, and HMBC (Figures S3−S5 in Supporting Information). In each of these spectra, the cross peaks corresponding to the major conformer $\mathbf{I_2}$ are readily distinguished from those of the minor conformers $\mathbf{II_1}$ and $\mathbf{III_2}$ on the basis of their intensities and positions. It was therefore possible to assign exact chemical shifts to every ^{1}H and ^{13}C nucleus for the $\mathbf{I_2}$ conformer. The connectivity was established using three-bond HMBC correlations to work from the end of the oligomer toward the center; sufficient separation is observed in the ^{13}C chemical shifts of the carbons along the biaryl backbone to make these assignments straightforward.

Using the EXSY spectrum, it was then possible to map these assignments from $\mathbf{I_2}$ onto $\mathbf{II_1}$ and $\mathbf{III_2}$. In other words, with exact ^{1}H assignments for conformer $\mathbf{I_2}$ in hand, the cross peaks in the EXSY spectrum allowed the minor signals in the ^{1}H NMR spectrum to be assigned to the analogous ^{1}H nuclei in conformers $\mathbf{II_1}$ and $\mathbf{III_2}$. These new assignments are further supported by weak COSY cross peaks between protons on individual arene rings within each minor conformer. This procedure allowed a complete, unambiguous set of ^{1}H chemical shift assignments to be obtained for $\mathbf{III_2}$. However, because the basis for our assignments is a conformer of 2-fold symmetry, there is some ambiguity to our assignments for the unsymmetric $\mathbf{II_1}$: although we obtain a set of assignments for each of the six distinct rings in $\mathbf{II_1}$, protons from the corresponding rings on either side of the oligomer cannot be distinguished since the symmetry has been lifted (i.e., ring 1 from 6, 2 from 5, 3 from 4). This discrepancy was addressed as discussed below. Complete chemical shift assignments for all conformers are given in the Supporting Information (Table S1).

Having obtained assigned sets of ^{1}H chemical shifts for all three conformers, we then required a way to associate them with specific molecular geometries. **oP^6** has three relevant degrees of conformational freedom: ϕ_2, ϕ_3, and ϕ_4. Application of the conformational analysis discussed above identifies six possible conformers. Four of these conformers are C_2-symmetric: AAA, ABA, BAB, and BBB. Two are C_1-symmetric (unsymmetric): AAB and BBA. Of these, AAA represents the closed helical conformer and BBB the open helical conformer. We carried out gas-phase geometry optimizations[24] for each conformer at the B3LYP/6-31G(d) level, with the resulting geometries shown in Figure 7. The methoxy groups in each case were oriented by choosing their lowest energy configuration, conforming to the backbone symmetry, as determined by a complete conformational search at the MMFF level prior to ab initio optimization.

NMR spectroscopy has been a powerful tool in the understanding of the conformational behavior of oligomeric systems in the past. Often, upfield shifts in the ^{1}H NMR signals for aromatic protons are taken as evidence for π-stacked conformations.[25] Further, NOESY correlations between remote sites on an oligomer provide strong direct evidence for specific folded conformations.[25c,d,26] Unfortunately, however, these approaches are not applicable to the **oP^n** series. For the *o*-phenylenes, all conformations consist of a high density of aromatic rings; thus, general statements with respect to differences in chemical shifts between conformations are impossible.

(21) Friebolin, H. *Basic One- and Two-Dimensional NMR Spectroscopy*, 4th ed.; Wiley-VCH: Weinheim, 2005.

(22) Some genuine NOESY signals, of opposite phase to the diagonal, are observed between the methoxy groups and the corresponding *ortho* aromatic protons (see Supporting Information).

(23) The EXSY spectrum of **oP^6** is reminiscent of that of 1,2,4,5-tetra(*o*-tolyl)benzene, which exhibits slow exchange between five atropisomers on the NMR time scale: Lunazzi, L.; Mazzanti, A.; Minzoni, M. *J. Org. Chem.* **2005**, *70*, 10062–10066.

(24) Frisch, M. J., et al. *Gaussian 03, revision D.02*; Gaussian, Inc.: Wallingford, CT, 2004.

(25) (a) Lokey, R. S.; Iverson, B. L. *Nature* **1995**, *375*, 303–305. (b) Nelson, J. C.; Saven, J. G.; Moore, J. S.; Wolynes, P. G. *Science* **1997**, *277*, 1793–1796. (c) Jiang, H.; Léger, J.-M. M.; Huc, I. *J. Am. Chem. Soc.* **2003**, *125*, 3448–3449. (d) Jones, T. V.; Slutsky, M. M.; Laos, R.; de Greef, T. F. A.; Tew, G. N. *J. Am. Chem. Soc.* **2005**, *127*, 17235–17240. (e) Ghosh, S.; Ramakrishnan, S. *Macromolecules* **2005**, *38*, 676–686. (f) Jiang, J.; Slutsky, M. M.; Jones, T. V.; Tew, G. N. *New J. Chem.* **2010**, *34*, 307–312.

(26) Gong, B.; Zeng, H.; Zhu, J.; Yuan, L.; Han, Y.; Cheng, S.; Furukawa, M.; Parra, R. D.; Kovalevsky, A. Y.; Mills, J. L.; Skrzypczak-Jankun, E.; Martinovic, S.; Smith, R. D.; Zheng, C.; Szyperski, T.; Zeng, X. C. *Proc. Natl. Acad. Sci. U.S.A.* **2002**, *99*, 11583–11588.

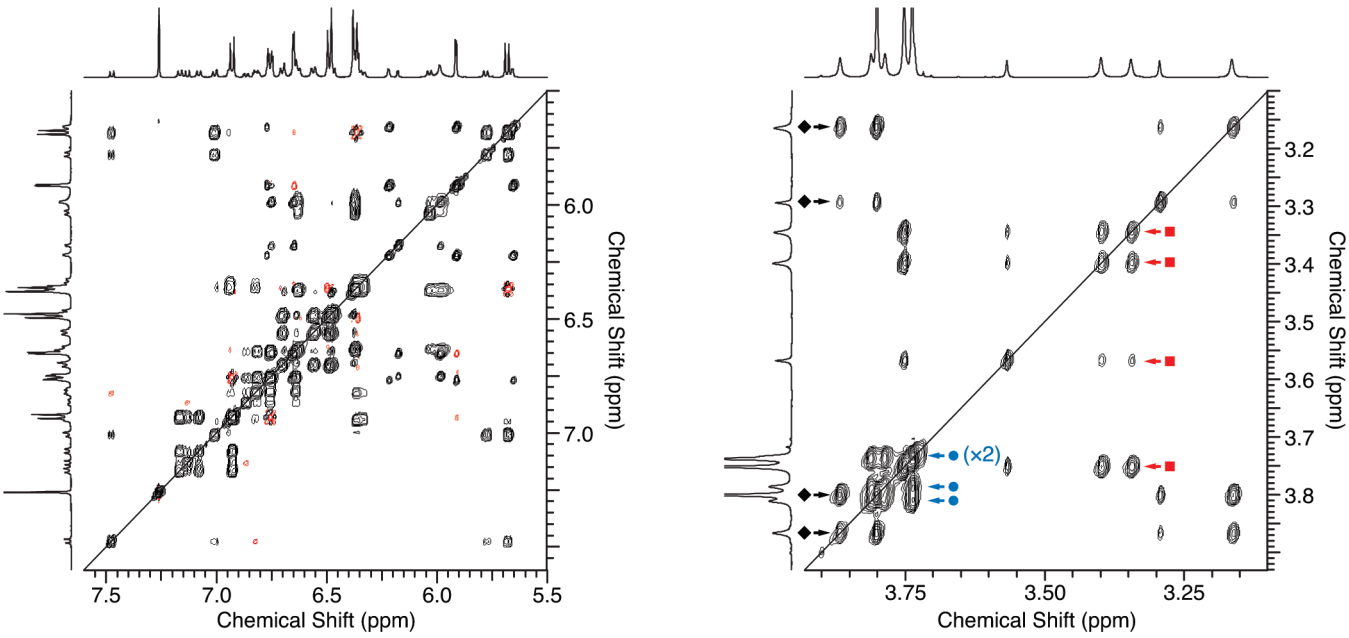

FIGURE 6. ^{1}H EXSY/NOESY spectrum of **oP^{6}** (500 MHz, $CDCl_3$, −5 °C, t_m = 0.5 s). Positive contours (EXSY) are shown in black, and negative (NOESY) in red. Left: aromatic region. Right: methoxy region; the arrows indicate the three different sets of methoxy groups (rings 3/4, black diamonds; rings 2/5, red squares; rings 1/6, blue circles).

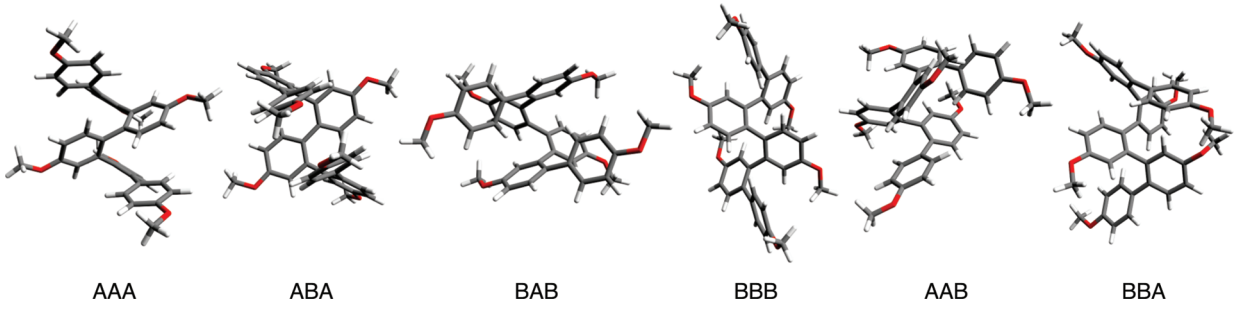

FIGURE 7. B3LYP/6-31G(d) minimized geometries of **oP^{6}** conformers.

In principle, NOESY correlations would be useful, but we were unable to observe any useful cross peaks in our spectra; some NOESY signals are present (Figures 6 and S2 in Supporting Information), but none relating protons that are at remote positions along the oligomer backbone.

However, it is clear from the experimental chemical shift assignments that the ^{1}H chemical shifts of **oP^{6}** are extremely sensitive to its conformational state, with great changes in shielding for some protons depending on their orientations relative to other nearby aromatic rings (and their associated ring currents). In one case, the chemical shift varies over almost 2 ppm between the three conformations (Table S1 in Supporting Information). Given this sensitivity, the *o*-phenylenes appeared to be excellent candidates for ab initio calculations of their NMR spectra. Theoretical predictions of NMR spectra are receiving increasing attention in the structure elucidation of stereoisomers[27] and in conformational analysis.[28] The **oP^{n}** system is ideally suited to these methods since it is focused on single conformers, and thus the calculated chemical shifts for multiple geometries do not need to be averaged based on their relative stability. Computational predictions of *proton* chemical shifts are well-developed, although not yet as broadly applied as those for the heavier nuclei (e.g., ^{13}C). To our knowledge, these methods have not yet been widely used in the conformational analysis of aromatic oligomers and nanostructures, although there are some reported examples.[29]

NMR spectral predictions for each of the optimized conformers of **oP^{6}** were carried out using density functional theory and the GIAO method.[30] Recently, Bally and Rablen demonstrated that accurate calculations of chemical shifts could be obtained using this approach even with relatively small basis sets, which was critical for this project given that

(27) Bifulco, G.; Dambruoso, P.; Gomez-Paloma, L.; Riccio, R. *Chem. Rev.* **2007**, *107*, 3744–3779.
(28) (a) Forsyth, D. A.; Sebag, A. B. *J. Am. Chem. Soc.* **1997**, *119*, 9483–9494. (b) Belostotskii, A. M. *J. Org. Chem.* **2008**, *73*, 5723–5731.
(29) (a) Peña, D.; Cobas, A.; Pérez, D.; Guitián, E.; Castedo, L. *Org. Lett.* **2003**, *5*, 1863–1866. (b) Kudo, M.; Hanashima, T.; Muranaka, A.; Sato, H.; Uchiyama, M.; Azumaya, I.; Hirano, T.; Kagechika, H.; Tanatani, A. *J. Org. Chem.* **2009**, *74*, 8154–8163. (c) Bharat; Bhola, R.; Bally, T.; Valente, A.; Cyrański, M. K.; Dobrzycki, Ł.; Spain, S. M.; Rempała, P.; Chin, M. R.; King, B. T. *Angew. Chem., Int. Ed.* **2010**, *49*, 399–402. (d) Miyasaka, M.; Pink, M.; Rajca, S.; Rajca, A. *Org. Lett.* **2010**, *12*, 3230–3233.
(30) (a) Ditchfield, R. *Mol. Phys.* **1974**, *27*, 789–807. (b) Wolinski, K.; Hinton, J. F.; Pulay, P. *J. Am. Chem. Soc.* **1990**, *112*, 8251–8260.

it focuses on large molecules (e.g., **oP^{12}**).[31] Following their recommendations, we carried out single-point calculations on the optimized gas-phase geometries of **oP^{6}** (Figure 7) using the 6-31G(d) basis set and the WP04 functional, which was specifically parametrized for the calculation of proton chemical shifts in chloroform.[32] Solvent effects were included in the calculations using the PCM-SCRF method.[33] For the purpose of visualization of the data, the isotropic shieldings were subtracted from that of TMS calculated at the same level.

For each candidate geometry (Figure 7), the calculated chemical shifts were then plotted against the sets of experimental values for conformers of equivalent symmetry. The best matches between the simulated molecular geometries and the experimentally assigned chemical shifts were then identified using linear regression. Since the intercept was allowed to vary, this method does not depend on the quality of the TMS reference value. As the figure of merit, we chose the standard error of the regression, s_e (i.e., the root-mean-squared residual).[34] This approach is essentially equivalent to the "scaled" method described by Bally and Rablen.[31] Since we were unable to unambiguously map the connectivity of **II$_1$** (see above), the experimental chemical shifts for the corresponding rings on either side of the oligomer were swapped such that they yielded the lowest s_e when compared to the calculated AAB and ABB chemical shifts. In other words, since we cannot distinguish rings 1 from 6, 2 from 5, and 3 from 4 in the experimental data, we choose the configuration that gave the lowest s_e. Since mismatches are more likely than the "true" match to generate falsely low values for s_e, this should constitute a conservative approach to judging the best match between the various calculated geometries and the experimental data for unsymmetrical conformers.[35]

Plots of the residuals arising from the linear regressions are shown in Figure 8, and the raw scatter plots are provided in the Supporting Information (Figure S6). For each conformer detected by NMR, the match between the experimental chemical shifts and those calculated for one specific geometry is visually obvious, both in the residual plots and in the raw scatter plots. The agreement between the experimental and predicted data for the good matches is striking, particularly given that we have considered only one possible arrangement of the methoxy groups. In general, we take s_e below 0.15 ppm to indicate a good match, and s_e greater than 0.35 ppm to indicate a poor match. No comparisons in this study have s_e values lying between these two thresholds, and in all cases only one geometry matches the experimental data.[36] More quantitatively, the s_e values were compared using a nonparameterized pseudo-F test (see Supporting Information for details). Statistically, the s_e values for the good matches are significantly smaller than those for the next best matches at confidence levels of at least 99.5%.

On the basis of these results, which explicitly considered every possible backbone conformation available to **oP^{6}**, we can make the following assignments. The major 2-fold-symmetric conformer **I$_2$** is the AAA conformer, accounting for approximately 55% of the total population. The unsymmetric conformer **II$_1$** is the AAB conformer, accounting for 36% of the population. The minor 2-fold-symmetric conformer **III$_2$** is the BAB conformer, accounting for 10% of the population.

Encouraged by these results, we applied the same strategy to the higher oligomers **oP^{8}**−**oP^{12}**. Like **oP^{6}**, each of the longer oligomers exhibits a principal 2-fold-symmetric conformer that dominates its ^{1}H NMR spectrum, with a number of smaller signals arising from slowly exchanging minor conformers. For each of the oligomers, we were able to obtain unambiguous ^{1}H and ^{13}C chemical shifts for this major conformer using a combination of DQFCOSY, HMQC, and HMBC experiments. We were then able to use the EXSY spectra to map the ^{1}H chemical shift assignments onto the most significant minor conformer, which is always unsymmetric. As before, because we are moving from higher to lower symmetry, the corresponding rings on opposite sides of the oligomer cannot be distinguished in the unsymmetric conformers using this approach. Experimental spectra and tables of assigned chemical shifts are given in the Supporting Information (Figures S7−S21 and Tables S2−S4).

Since the number of possible conformers available to the oligomers increases greatly with increasing n, it was impractical to carry out computational NMR predictions for every possible candidate. Instead, for each case we considered three conformers of C_2 symmetry and three of C_1 symmetry (Figures S22−S24 in Supporting Information). MMFF conformer distributions were used as guides for selection. For the C_2-symmetric conformers, these calculations always identified the closed helix (A_{n-3}) as the most stable. We then included the second-lowest energy 2-fold-symmetric conformer and, because of its significance as the major conformer of the poly(2,3-quinoxaline)s, the open helix (B_{n-3}) as well. Similarly, we chose the three lowest energy C_1 conformers, which with the exception of **oP^{12}** included a closed helical conformer with a single defect at the end, $A_{n-4}B$ (for **oP^{12}**, we selected the two lowest energy C_1 conformers plus $A_{n-4}B$). Admittedly, the MMFF method is unlikely to produce high quality estimates of the relative stability of these different geometries. However, this approach was systematic and, taken as a whole, provided a good selection of conformers with a comprehensive set of structural changes, including variations in ϕ_i at the ends (e.g., BA_5B, A_5B_2) and in the center (e.g., $A_3B_4A_2$) of the chains relative to the stacked helical conformers. As for **oP^{6}**, the methoxy groups for each backbone conformation were oriented according to their lowest energy MMFF configuration, and the geometries minimized at the B3LYP/6-31G(d) level.

NMR chemical shifts were again predicted at the GIAO-PCM-WP04/6-31G(d)//B3LYP/6-31G(d) level for each candidate geometry. These predictions were then matched

(31) Jain, R.; Bally, T.; Rablen, P. R. *J. Org. Chem.* **2009**, *74*, 4017–4023.
(32) Wiitala, K. W.; Hoye, T. R.; Cramer, C. J. *J. Chem. Theory. Comput.* **2006**, *2*, 1085–1092.
(33) Cossi, M.; Scalmani, G.; Rega, N.; Barone, V. *J. Chem. Phys.* **2002**, *117*, 43–54.
(34) $s_e = \sqrt{\frac{\sum_i (y_i - \hat{y}_i)^2}{N-2}}$ where $y_i - \hat{y}_i$ is the i^{th} residual and N is the total number of data points.
(35) In general, we find very good correspondence between the calculated and experimental chemical shifts for the unambiguous case of the C_2-symmetric conformers. Thus, we can be reasonably confident that for the proper match to the C_1-symmetric conformer, minimization of s_e will lead to the correct assignments. In the case of mismatches, it is quite possible that random errors will cause us to improperly exchange the shifts for one or more of the ambiguous rings as we minimize s_e. Thus, s_e values for mismatches may be falsely low; however, the s_e values for the matches themselves should be correct, and the overall comparison (based on F; i.e., the ratio of s_e^2 values) should be conservative.
(36) The 0.15 ppm cutoff is in good agreement with the root mean squared error (0.120 ppm) originally reported for this method using the standardized test set of very different compounds, ref 31.

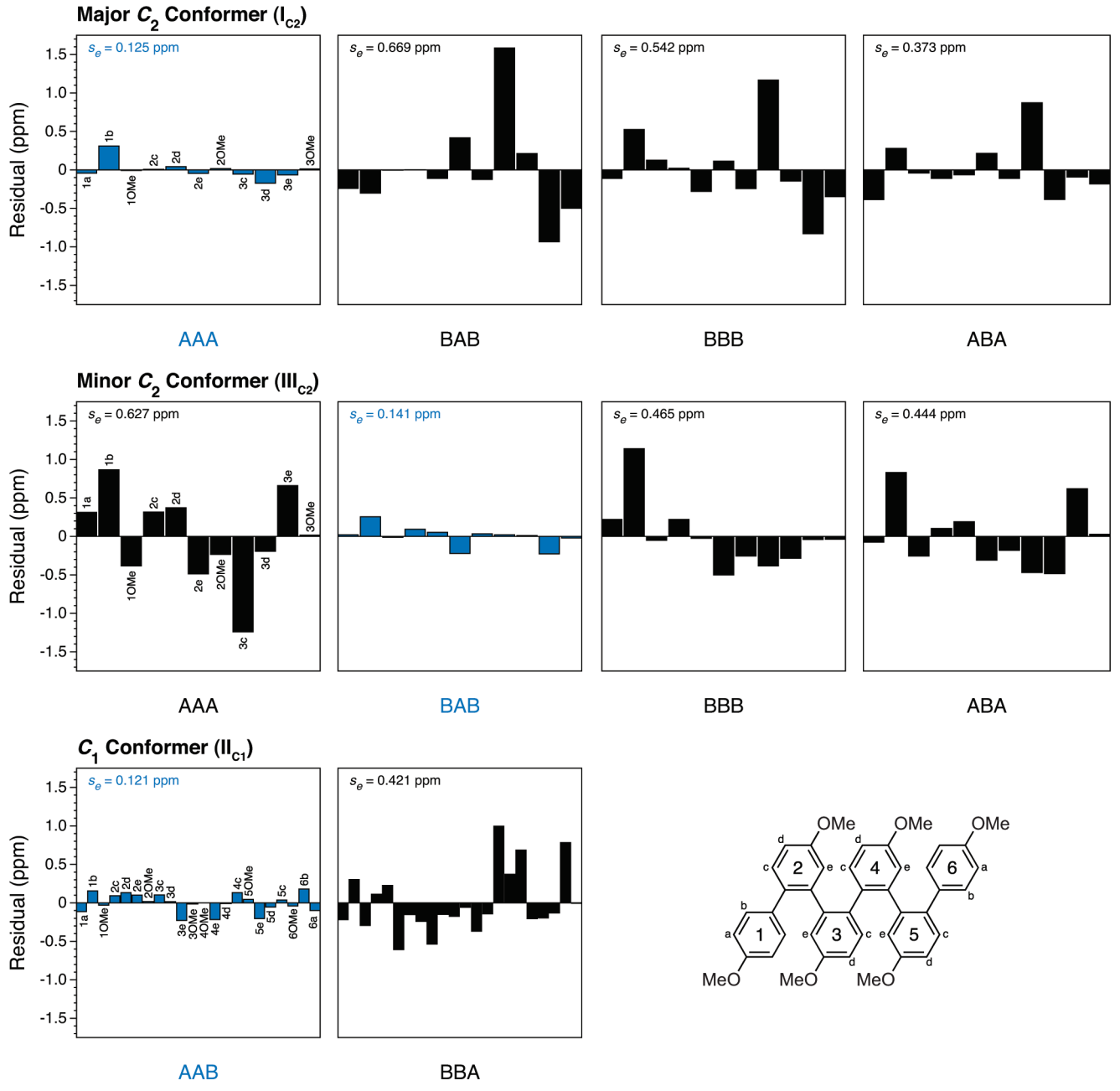

FIGURE 8. Linear regression residuals of calculated GIAO-PCM-WP04/6-31G(d)//B3LYP/6-31G(d) ^{1}H NMR chemical shifts plotted versus experimental values for all six possible **oP^6** conformers. The best matches between the experimental and calculated data are colored blue.

to the experimentally determined chemical shifts for the two conformers using the s_e values extracted from a linear fit of calculated versus experimental data (Figures S25−S27 in Supporting Information). A complete list of the conformers examined and their match with the experimental results is given in Table 1. Without exception, the major 2-fold-symmetric conformer identified by NMR corresponds to the closed helix A_{n-3}, and the minor unsymmetric conformer corresponds to $A_{n-4}B$. In all cases, the s_e values for the good matches are statistically less than those for the next-best matches with at least 99.8% confidence. On the basis of peak fitting and deconvolution of the methoxy region of the ^{1}H NMR spectra, the major conformer typically accounts for approximately 50% of the total population, and the less significant conformer 25%. The optimized geometries for these conformers are given in Figure 9.

Since the fully closed helical conformer, A_{n-3}, predominates in all cases, it is clear that the conformational behavior of the **oP^n** series is dominated by the $\phi_i = 70°$ ("A") state, as was suggested in our previous paper. Further, it appears that defects in the helix, the $\phi_i = 130°$ ("B") state, are largely localized at the ends of the oligomer, since in all cases the $A_{n-4}B$ conformer is the second-most populated. For all oligomers considered, the A_{n-3} and $A_{n-4}B$ states combined account for at least 70% of the total population. Presumably, a significant number of the remaining unassigned signals arise from the C_2-symmetric $BA_{n-5}B$ conformer (as was experimentally confirmed for **oP^6**); thus, it appears that

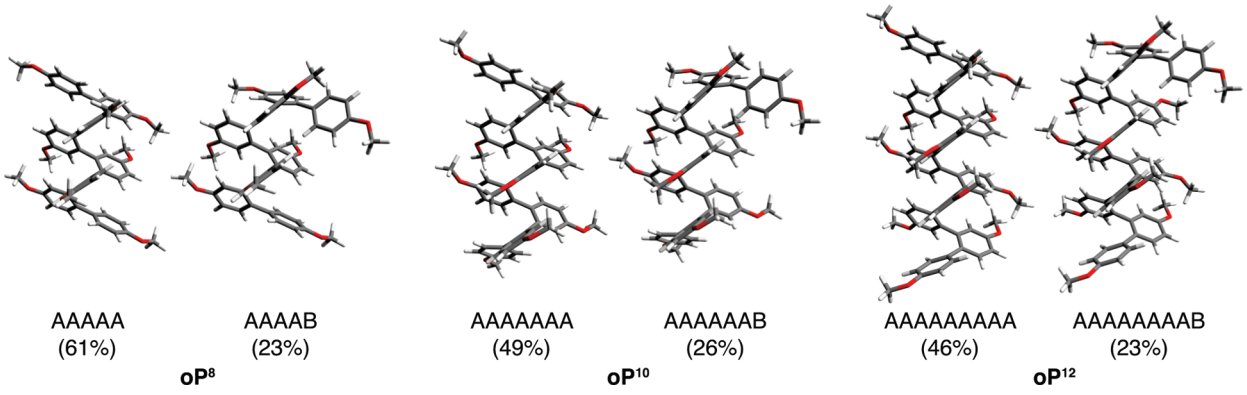

FIGURE 9. Lowest energy conformations identified for **oP^8**, **oP^{10}**, and **oP^{12}**. The numbers in parentheses correspond to their proportion of the total population as determined by NMR integration.

TABLE 1. Conformations of oP^n and Comparisons to Experimental NMR Data

oP^n	conformation	symmetry	%[a]	s_e[b]	rel E[c] (kcal/mol)
oP^6			**55**	**0.125 (I_2)**	
	AAA	C_2		0.627 (III_2)	0.8
				0.669 (I_2)	
	BAB	C_2	**10**	**0.141 (III_2)**	0.0
				0.373 (I_2)	
	ABA	C_2		0.444 (III_2)	12.4
				0.542 (I_2)	
	BBB	C_2		0.465 (III_2)	0.6
	AAB	C_1	**36**	**0.121 (II_1)**	0.7
	BBA	C_1		0.421 (II_1)	4.2
oP^8	**AAAAA**	C_2	**61**	**0.100**	2.0
	BAAAB	C_2		0.544	0.1
	BBBBB	C_2		0.534	0.0
	AAAAB	C_1	**23**	**0.133**	0.8
	AAABB	C_1		0.398	0.1
	AABBA	C_1		0.447	2.8
oP^{10}	**AAAAAAA**	C_2	**49**	**0.108**	2.8
	BAAAAAB	C_2		0.499	1.5
	BBBBBBB	C_2		0.561	0.0
	AAAAAAB	C_1	**26**	**0.130**	2.0
	AAABBAA	C_1		0.469	0.2
	AAAAABB	C_1		0.322	1.2
oP^{12}	**AAAAAAAAA**	C_2	**46**	**0.107**	6.0
	AABBBBBAA	C_2		0.474	1.7
	BBBBBBBBB	C_2		0.575	1.2
	AAAAAAAAB	C_1	**23**	**0.136**	5.6
	AAAABBAAA	C_1		0.460	2.9
	AAABBBBAA	C_1		0.452	0.0

[a]Estimated percentage of the total population at −5 °C, as determined by peak fitting and deconvolution of the methoxy region of the NMR spectrum. [b]Best matches indicated in boldface. [c]Relative gas-phase energies calculated at the B3LYP/6-31G(d) level, including zero-point correction.

the population of **oP^n** molecules is best described as stacked helices, with defects occurring primarily at the ends. This suggests that the *o*-phenylene motif may indeed be a promising means to organize the constituent monomers into well-defined three-dimensional structures, allowing the repeat units to be ordered into stacked arrangements. In the case of simple benzene-based monomers (i.e., the **oP^n** series), spatial overlap is somewhat limited, although there are some very close contacts (ca. 3.4 Å between the closest atoms). Repeat units with larger π-surfaces should exhibit better through-space interactions. Once these materials are synthesized, the current strategy affords a general method to establish their conformational state in solution.

What is the origin of this preference for the closed helical conformation? According to the relative gas-phase energies calculated at the B3LYP/6-31G(d) level (Table 1), the A_{n-3} states are actually predicted to be slightly *less* stable than most of the other conformers that were considered (although it is interesting to note that the closed conformation is usually the global minimum by MMFF).[37] Within this context, it is remarkable that the closed helical conformation is so prevalent. For example, for **oP^{12}** there are 32 possible symmetrical and 240 possible unsymmetrical conformers (see Supporting Information). Of these 272 possibilities, A_9 and A_8B account for roughly 70% of the total population. Solvophobicity is unlikely to be a significant factor, since chloroform is typically a good solvent for aromatic oligomers, promoting random coil conformations in a variety of non-hydrogen-bonded systems,[25b,d] including the *m*-phenylenes.[11d] Further, in our previous study we observed essentially no solvatochromism in the UV−vis and fluorescence spectra of the **oP^n** series, suggesting that the conformational behavior is not strongly solvent-dependent. It therefore appears likely that the bias toward the closed helix is due to torsional preferences that are not captured in the gas-phase DFT calculations. For example, the B3LYP/6-31G(d) level is unlikely to accurately estimate the energetic contribution of any favorable arene−arene interactions that could contribute to the overall stability of stacked helical conformations.[38] However, we cannot at this point eliminate other effects, such as the minimization of excluded volume.[39]

Beyond the relevance of our results to *o*-phenylenes specifically, we believe that one of the most important aspects of this study is the illustration of the utility of relatively low-cost GIAO ^{1}H NMR chemical shift calculations in the determination of the solution-phase conformational behavior of aromatic nanostructures. All of the calculations described in this paper were performed on single two-processor computational nodes that are no more powerful than a typical

(37) For **oP^6**−**oP^{10}**, the closed helix is indeed identified by MMFF as the most stable conformer. For **oP^{12}**, it is the most stable C_2-symmetric conformer.

(38) (a) Godfrey-Kittle, A.; Cafiero, M. *Int. J. Quantum Chem.* **2006**, *106*, 2035–2043. (b) Tsuzuki, S.; Lüthi, H. P. *J. Chem. Phys.* **2001**, *114*, 3949–3957.

(39) Snir, Y.; Kamien, R. D. *Science* **2005**, *307*, 1067–1067.

(40) The most demanding calculations take on the order of days to weeks to complete. While we obtained the best results using the WP04 functional using Gaussian 03, the performance of GIAO calculations as implemented in Spartan 08 (B3LYP/6-31G(d), gas-phase) was quite acceptable when tested with some of these geometries.

desktop computer.[40] Other architectures with a high density of aromatic rings should be very well suited to this method given the sensitivity of their proton chemical shifts to the specific conformational state, which is already well-documented as large upfield shifts in stacked conformations. This method provides a good complement to other methods based on shifts in electronic spectra or the observation of NMR NOE correlations. It is, however, most appropriate for applications where chemical changes can be assigned to specific conformers or to small populations of rapidly exchanging conformers with readily estimated relative stability.

Conclusions

In summary, we have used a combination of NMR spectroscopy and ab initio calculations to determine the conformational behavior of a series of *o*-phenylenes. For the shortest oligomer, **oP^6**, we have explicitly considered every possible backbone conformer, whereas for the longer oligomers (**oP^8**−**oP^{12}**) subsets of six conformers were considered on the basis of MMFF energy minimizations. We have found that these oligomers adopt well-defined, stacked helical conformations in solution, with some disorder at the ends. This suggests that torsional biases in the *o*-phenylene motif may offer a general method to organize arene repeat units in three dimensions. Our results also illustrate the potential of GIAO calculations of ^{1}H NMR spectra as a tool for the determination of the conformational behavior of oligomers in solution, especially when they incorporate a high density of aromatic rings.

Experimental Section

The synthesis of **oP^6**−**oP^{12}** has been reported previously.[16] NMR spectra were acquired on a 500 MHz spectrometer using standard pulse sequences. Chemical shifts are referenced to the residual $CHCl_3$ as an internal standard (7.26 ppm vs TMS). Measured temperatures are uncorrected. Pulse widths were calibrated before each experiment. All NMR spectra were processed using ACD/Labs NMR Processor (v. 12), which allows overlapping peaks to be deconvoluted for integration. Conformational analysis was carried out using Spartan 08 (v. 1.1.1) on a standard PC laptop computer. Gaussian 03 (Rev. D.02) calculations were carried out on Miami University's Redhawk computer cluster. Following geometry optimizations, frequency analysis was used to determine zero-point corrections and to ensure that all stationary points were energy minima. The WP04 functional is invoked by using the BLYP functional along with a IOp(3/76 = 1000001189, 3/77 = 0961409999, 3/78 = 0000109999) keyword. In some cases, the NoSymmCav option was required for the SCRF-PCM method to avoid errors in solvent cavity generation, as was reported by Bally and Rablen.[31]

Acknowledgment. This work was supported by the National Science Foundation (CHE-0910477), Miami University, and the donors of the American Chemical Society Petroleum Research Fund (47926-G7). We thank Prof. Blanton S. Tolbert for helpful discussions and Prof. Michael Novak for a critical reading of the manuscript.

Supporting Information Available: Complete 1D ^{1}H NMR spectra, EXSY/NOESY spectra, DQFCOSY spectra, HMQC spectra, HMBC spectra, tables of ^{1}H and ^{13}C chemical shifts, plots of calculated vs experimental chemical shifts, optimized conformer geometries of **oP^8**−**oP^{12}**, description of statistical analysis, calculation of the number of possible conformers for **oP^n**, complete ref 24, and Cartesian coordinates of all optimized geometries. This material is available free of charge via the Internet at http://pubs.acs.org.